Journal of Biomimetics, Biomaterials and Biomedical Engineering
ISSN: 2296-9845, Vol. 41, pp 69-81
doi:10.4028/www.scientific.net/JBBBE.41.69

Submitted: 2019-01-11
Revised: 2019-03-23
Accepted: 2019-03-26
Online: 2019-04-22

CNT Incorporated Polyacrilonitrile/Polypyrrole Nanofibers as Keratinocytes Scaffold

Atike Ince Yardimci[1,a*], Hande Aypek[2,b], Ozgur Ozturk[2,c], Selahattin Yilmaz[3,d], Engin Ozcivici[4,e], Gulistan Mese[2,f] and Yusuf Selamet[5,g]

[1]Department of Material Science and Engineering, Izmir Institute of Technology, Urla, İzmir, Turkey

[2]Department of Molecular Biology and Genetics, Izmir Institute of Technology, Urla, İzmir, Turkey

[3]Department of Chemical Engineering, Izmir Institute of Technology, Urla, İzmir, Turkey

[4]Department of Bioengineering, Izmir Institute of Technology, Urla, İzmir, Turkey

[5]Department of Physics Izmir Institute of Technology, Urla, İzmir, Turkey

[a*]atikeince@gmail.com, [b]handeaypek@iyte.edu.tr, [c]ozgurozturke@gmail.com, [d]selahattinyilmaz@iyte.edu.tr, [e]enginozcivici@iyte.edu.tr, [f]gulistanmese@iyte.edu.tr, [g]yusufselamet@iyte.edu.tr

Keywords: Polypyrrole, carbon nanotube (CNT), electrospinning, biocompatibility, keratinocyte.

Abstract. Polypyrrole (PPy) is an attractive scaffold material for tissue engineering with its non-toxic and electrically conductive properties. There has not been enough information about PPy usage in skin tissue engineering. The aim of this study is to investigate biocompatibility of polyacrilonitrile (PAN)/PPy nanofibrous scaffold for human keratinocytes. PAN/PPy bicomponent nanofibers were prepared by electrospinning, in various PPy concentrations and with carbon nanotube (CNT) incorporation. The average diameter of electrospun nanofibers decreased with increasing PPy concentration. Further, agglomerated CNTs caused beads and disordered parts on the surface of nanofibers. Biocompatibility of these PAN/PPy and PAN/PPy/CNT scaffolds were analyzed in vitro. Both scaffolds provided adhesion and proliferation of keratinocytes. Nanofiber diameter did not significantly influence the morphology of cells. However, with increasing number of cells, cells stayed among nanofibers and this affected their shape and size. In this study, we demonstrated that PAN/PPy and PAN/PPy/CNT scaffolds enabled the growth of keratinocytes, showing their biocompatibility.

1. Introduction

Electrospun polymer nanofibers are important scaffold components for tissue engineering as they can be engineered to biomimic the 3D organization of the extracellular matrix (ECM) [1-3]. Electrospun fibrous scaffolds can be optimized in mechanical, chemical and degradative properties that can greatly influence their interaction with cells [4] and their high surface area and porosity provide attachment and migration of cells within the scaffold [5]. To date, various electrospun polymers have been investigated as scaffold materials for different cell types such as smooth muscle and endothelial cells, bone cells, skeletal cells [5-12].

Polypyrrole (PPy) is a unique biocompatible polymer that is conductive with physiological level actuation voltages [13]. PPy films treated with different ECM components were found to support skeletal myoblast proliferation, adhesion and differentiation [8]. PPy films and nanofibers were utilized in artificial muscle with physiological actuation (< 2V) and were capable of reaching active stress and strain levels up to 30 MPa and 39% [10, 11, 14]. PPy was found to give the largest stroke value among the conducting polymers for electrochemical actuation [12]. Fabrication of nanofiber PPy is also possible and composite electrospun PPy nanofibers were already shown to be an appropriate scaffold material for biomedical applications [6, 7]. In a cardiac tissue engineering application, conductive PPy/PCL/gelatin electrospun nanofibrous scaffolds promoted cell attachment, proliferation, and expression of cardiac specific proteins [6]. Furthermore, PPy–PLGA fibers were shown to be suitable candidates of neural tissue applications with both passive

topographical guidance and active permissibility to electrical stimulation [7]. Along with its composite applications with other polymers, PPy matrices can also be reinforced with various components including sulphur nanowires [15], graphene [16] and carbon nanotubes [17].

Carbon nanotubes (CNTs) have attracted considerable attention based on their excellent electrical and mechanical properties [18]. By incorporating CNTs to PPy, its electrical, mechanical and electrochemical properties can be improved, leading to increased actuation response and reduced actuation voltages [19, 20]. Another influence of CNTs on the polymer matrix is an elevation of actuation strain and conductivity, increasing electrochemical efficiency [21]. These properties aggregate to CNTs importance in tissue engineering applications in addition to cell tracking, drug delivery, microenvironment sensing and providing structural support [22]. Though PPy / CNT composite can be readily fabricated [23], poor solubility of the composition is a limiting factor for electrospinning applications. This limiting factor for electrospun nanofiber fabrication can be alleviated by the utilization of polyacrylonitrile (PAN) as a co-polymer in the composition [24].

In this study, we tested PPy/PAN/CNT electrospun nanofibers as a potential scaffold material for skin tissue engineering applications. Though other polymer nanofibers have been tested as skin scaffolds such as PVA [25], chitin [26], silk [27], chitosan-gelatin [28], PLAGA poly(lactic acid-co-glicolic acid) [29], the applicability of conductive polymer nanocomposites were never studied previously. Our results indicated that PPy/PAN/CNT nanofibers provided a suitable scaffold material for keratinocyte growth.

2. Materials and Methods

2.1. Materials

To fabricate electrospun nanofibers PPy (Aldrich, Cat# 482552) was used with PAN (Aldrich, Cat# 181315) as a co-polymer to increase the solubility of PPy and N,N-dimethylformamide (DMF) (Aldrich, Cat# D158550) was used as a solvent.

Immortalized keratinocyte (HaCaT) cells were grown in Dulbecco's Modified Eagle Medium (DMEM, GIBCO, Cat# 41966-029) supplemented with 10% fetal bovine serum (FBS) and 1% penicillin/streptomycin. HaCaTs were replated by first incubating with EDTA (BI, Cat# 03-015-1B) for 20 min and then, 0.05% Trypsin/EDTA (BI, Cat# 03-053-1B) was applied to cells for 2 min at 5% CO_2 and 37 ^oC incubator. HaCaT cells were maintained in 5% CO_2 and 37 ^oC conditions.

2.2 PAN/PPy uniform and composite nanofiber synthesis

In order to prepare electrospinning solution, 8 wt% PAN was dissolved in DMF until a clear solution was obtained through mechanical stirring. Then, PPy was added to the PAN solution in DMF and stirred for 72 h at 60 ^oC. For this study we prepared 10 and 25 wt% PPy of total polymer. For composite nanofibers, 1 wt% CNT was added to PAN/PPy solution and dispersed by using ultrasonic bath for 24 h.

Obtained solutions were filled in a 20 ml syringe connected to a high voltage for electrospinning. For all samples 15 kV voltage was applied to the syringe and flow rate of solution was kept at 1.5 ml/h. The distance between the syringe and collector was 30 cm and the fibers were collected on 10 mm diameter cover slips which were fixed on Al foil for 1 hour. The polymer ratio that was used in the solution kept constant after evaporation of solvent (DMF) under electrical field and so it is the same ratio in the electrospun fibers. CNT incorporated PPy was prepared only for 10 wt% PPy, since solution containing 25 wt% PPy could not be electrospun when CNT was added to the solution.

Morphology of nanofibers was characterized by scanning electron microscopy (SEM, FEI Quanta-250FEG ESEM) at an acceleration voltage of 5 kV. Thermal behavior of nanofibers was determined by thermogravimetric analysis (TGA, Perkin Elmer-Diamond TGA) in the temperature range of 25-800 ^oC in air atmosphere at a heating rate of 10 ^oC/min.

Electrochemical measurements of the nanofibers were performed with cyclic voltammetry (CV) and electrochemical impedance spectroscopy (EIS) techniques. The same 3-electrode electrochemical cell was utilized for both techniques including a graphite working electrode covered

with our PAN/PPy nanofibers during electrospinning process, an Ag/AgCl reference electrode and a Pt wire counter electrode. The electrolyte solution was 0.1 M HCl solution for CV and Fe[CN6]3-/4 solution for EIS.

2.3 Cell culture and seeding

The cover slips with electrospun nanofibers were sterilized at 200 ^{o}C for 2h and were then placed in 12-well tissue culture plates where 25,000 HaCaT cells/well were plated on fibers for experiments.

2.4 Characterization of cell morphology by SEM

After 1, 3 and 7 days of culture, morphology of cells were analyzed with SEM. Cells were washed with phosphate-buffered saline (PBS) and then fixed with paraformaldehyde for 3-4 h at room temperature. After PBS washes, cells were air dried. Dry cellular constructs were sputter coated with gold and observed under the SEM at an accelerating voltage of 5 kV.

2.5 Immunostaining of keratinocytes

Cellular morphology of HaCaT on PAN/PPy electrospun nanofibers was investigated by immunostaining of actin cytoskeleton with Alexa Fluor 488 Phalloidin. Cells were washed with 1X PBS and then fixed with 4% paraformaldehyde (PFA) for 20 min, permeabilized with 0.1% Triton-X 100 for 15 min and blocked with 5% bovine serum albumin (BSA) for 1 h at room temperature (RT). Then, cells were incubated with a 1:200 dilution of Alexa Fluor 488 Phalloidin (Invitrogen, Cat# A12379) and DAPI (1:200) (Sigma, Cat# D95242) for 45 min at RT in dark. After washing with PBS, coverslips were dipped in distilled water, dried and mounted on glass slides. Staining was verified under a fluorescence microscope (IX83, Olympus, Japan) with 40x objective and images were taken with a CCD digital camera.

2.6 MTT assay

10,000 HaCaT cells were seeded onto PAN/PPy/CNT nanofibers in 12-well tissue culture plates (n=4 per condition). Cells were incubated at 37 ^{o}C and 5% CO_2. Medium was removed and 600 µl 10% MTT solution was added onto cells. After 4 hours of incubation, MTT mixture was removed and 600 µl of DMSO was added. After solubilization of MTT crystals, absorbance was measured at 570, 650 and 670 nm with Thermo Scientific Multiskan Spectrum. MTT measurements were performed at day 1, 3 and 7.

3. Results and Discussion

3.1 PAN/PPy nanofibers characterization

The morphology of electrospun PAN/PPy bicomponent nanofiber scaffolds were straight and randomly oriented, no bead formation was observed on nanofibers (Figure 1). Increasing PPy content resulted in an increase in solution conductivity and a decrease in solution viscosity, therefore producing nanofibers with smaller diameters [30]. The average diameter of electrospun nanofibers were 197 nm (Figure 1a) and 112 nm (Figure 1b) for 10 wt% and 25 wt% PPy concentration, respectively.

The average fiber diameter for sample containing 10 wt% PPy and 1 wt% CNT was 97 nm (Figure 1c). At low PPy concentration, surface morphology of nanofibers was smooth. Irregularities were observed with increasing PPy content. PAN improved the poor solubility of PPy and therefore the surface roughness of PPy fibers improved at low PPy concentrations [24]. CNT incorporation into nanofibers provided smaller diameter nanofibers because of increasing solution conductivity. Kaur et al. also observed decrease in nanofiber diameter for PAN/CNT nanofibers with addition of CNTs and increasing CNT concentration in PAN solution [31]. Besides, our results showed that number of beads increased due to agglomerated CNTs and the number of disordered nanofibers increased.

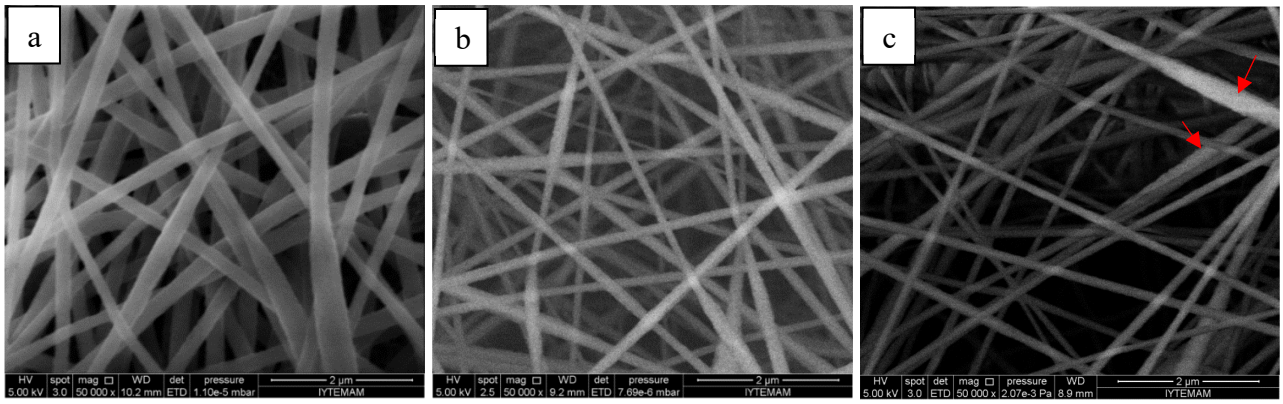

Figure 1 SEM micrographs of electrospun PAN/PPy nanofibers containing (a) 10 wt%, (b) 25 wt% PPy, (c) 10 wt% PPy with 1 wt% CNT. Scale bars 2µm.

Based on TGA curves, all nanofibers exhibited a degradation step corresponded to the removal of water in the temperature range of 50-130 ºC. Majority of the weight loss for pure PAN (0% PPy) nanofibers were observed at 310 and 500 ºC (Figure 2.a). PAN/PPy nanofibers containing 10 wt% PPy showed nearly the same decomposition characteristics with neat PAN (0 wt% PPy) nanofibers, even though the decomposition temperatures of pure PPy in air atmosphere were at 210 and 410 ºC [24]. Decomposition of nanofibers containing low PPy concentration was higher than the sample with high PPy concentration, due to easier phase degradation of PPy than PAN phase in air environment [32]. Nanofibers containing 25 wt% PPy however, decomposed between the decomposition temperatures of two polymers. In literature, PAN/PPy electrospun nanofibers were synthesized with 5, 10,15,30 and 50 wt% PPy ratios and their TGA results were agree with our results and indicated that 280 ºC was an appropriate stabilization temperature for PAN/PPy bicomponent nanofibers [24].

XRD observed patterns from PAN/PPy nanofibers displayed peaks that belong to (200) and (020) crystal planes at 17.19º and 29.95º, respectively (Figure 2.b). (020) plane peak indicated the difference in PAN conformation among the PAN samples; PAN nanofibers showed a peak at 2θ angle of 17.19º [33] while the cast PAN film and raw PAN powder gave peaks at 2θ angle of 16.92º and 16.79º, respectively [34]. However, for neat PAN nanofibers, we did not observe any peaks at (200). (200) and (020) plane peaks intensified with the increasing PPy content. At 25 wt% PPy concentration, a small and broad peak was observed at 24° due to the amorphous structure of the PPy due to the scattering of PPy from all over chains based on its amorphous structure [35, 36].

CV graphs of nanofibers containing 10 and 25 wt% PPy showed two oxidation waves at 0.2 and 0.7 V and one reduction wave approximately at 0.45 V (Figure 3). Output current, which is a direct indicator of conductivity of PAN/PPy nanofibers increased with increasing PPy amount from 10 to 25 wt%. Addition of CNTs also improved the conductivity of the nanofibers and exhibited well defined oxidation-reduction processes for PAN/PPy nanofibers. It indicated more effective ion exclusion/incorporation during oxidation and reduction which was very important for actuation properties of these nanofibers. Similar effects of CNT incorporation on polyaniline fibers electrochemical properties was reported previously [37]. However, the highest output current was observed for PAN/PPy nanofibers containing 25 wt% PPy. Thus, we can conclude that addition of CNT and PPy into the nanofibers made them electrically conductive (Nanofiber synthesis with 25 wt% PPy including CNTs was tested, but this solution could not be electrospun due to very high conductivity). CV results indicated that these nanofibrous scaffolds were electroactive and can be used as an electrochemical actuator in acidic solutions. The impedance value of nanofibers calculated from Nyquist plots were 1688 and 1066 ohm for PPy ratios of 10 and 25 respectively. CNT addition decreased the impedance value from 1688 to 1481 ohm for the nanofibers containing 10 wt% PPy. Low impedance value for CNT embedded PPy in film form was previously reported for PPy/CNT films synthesized chemically and electrochemically [38]. Increasing PPy and CNT addition decreased resistance and improved electrical properties of nanofibers. It indicated that highest recorded conductivity was obtained for nanofibers containing 25 wt% PPy.

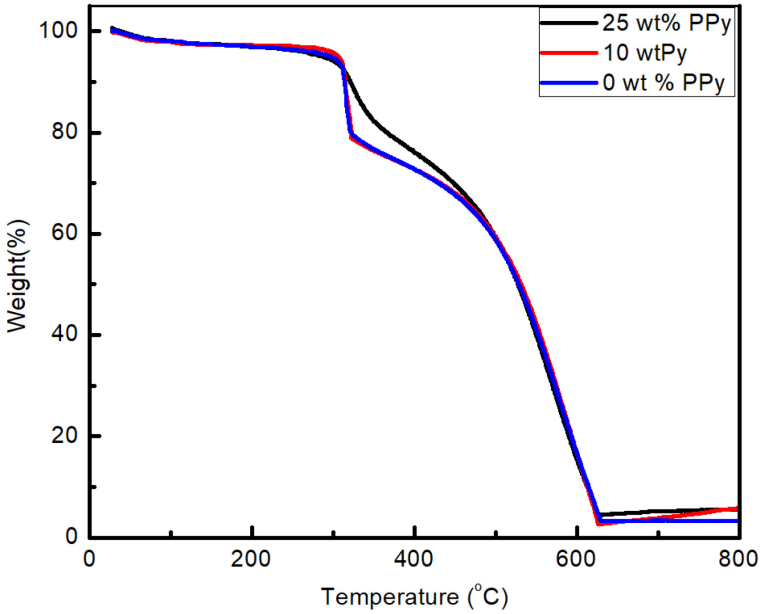

(a)

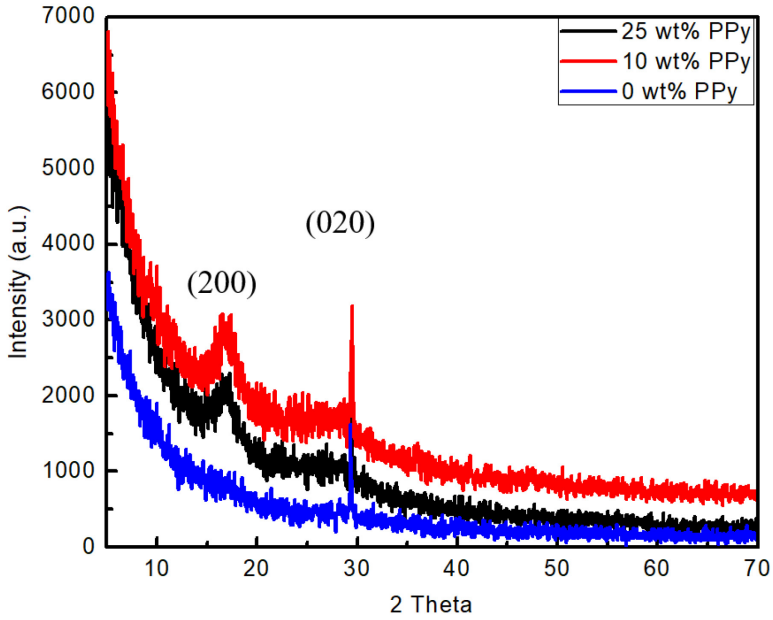

(b)

Figure 2 (a) TGA thermograms (b) XRD scans of electrospun PAN/PPy nanofibers containing 0 wt%, 10 wt% and 25 wt% PPy.

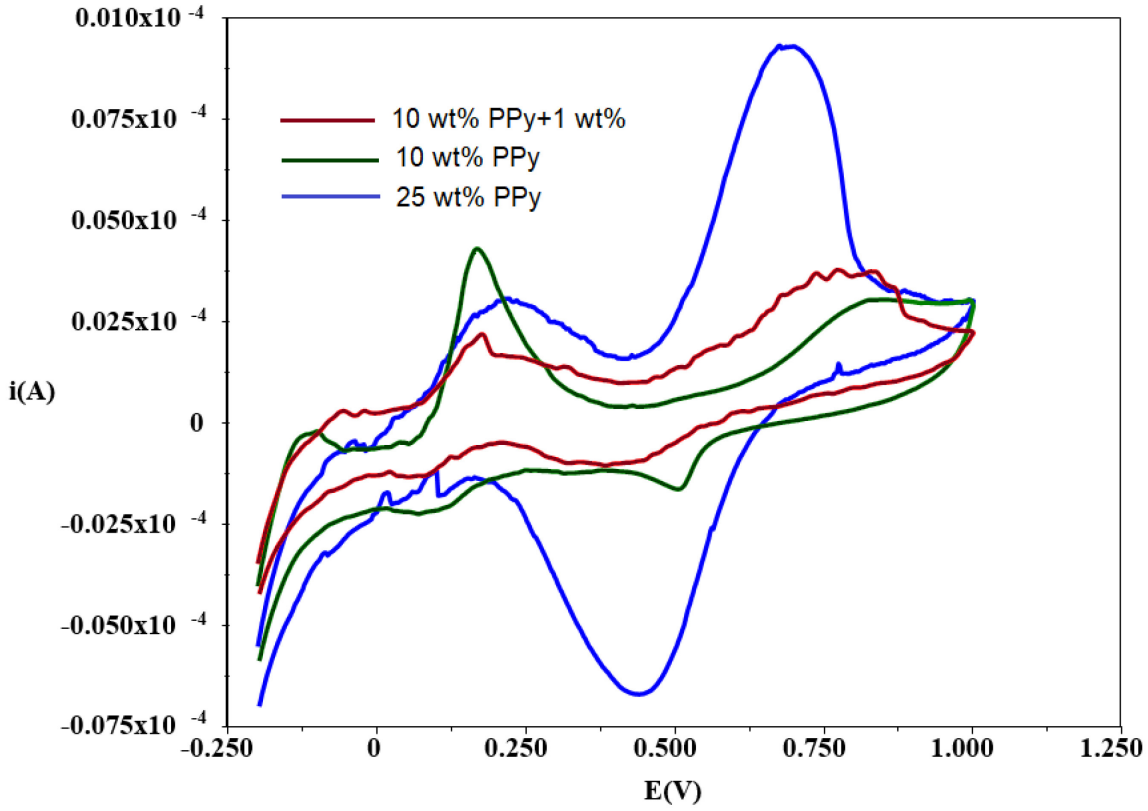

Figure 3 Cyclic voltammograms of electrospun PAN/PPy nanofibers containing 10 wt% and 25 wt% PPy, and 10 wt% PPy with 1 wt% CNT.

3.2 PAN/PPy and PAN/PPy/CNT electrospun nanofibers as a keratinocyte scaffold

Morphology of keratinocytes (HaCaT) and their interaction with PAN/PPy nanofibrous scaffold were observed during 7 days of growth using SEM (Figure 4). At the 1st day of culture, keratinocytes were observed to be attached on PAN/PPy scaffolds. Cells were able to proliferate on these scaffolds and formed colonies on 3rd and 7th days of culture (Figure 4 b and c). These suggested that keratinocytes were able to adhere and proliferate on PAN/PPy scaffolds.

Our data indicated that with increasing PPy concentration, fiber diameter was reduced (Fig. 1). In Fig. 4d, 4e, 4f, SEM pictures of cells seeded on nanofibers containing 25 wt% PPy showed that cells attached and spread on the fibers. It suggested that diameter of fibers did not influence the cell attachment and proliferation. The cell morphology was similar to cells seeded on scaffold containing lower PPy concentration. These suggested that PAN/PPy nanofibers interacted well with the skin cells. Guetta-Terrier et al. studied diameter effect of electrospun PCL scaffold and indicated that diameter range between 0.3 and 1.3 μm did not affect cell behavior [39]. However, in another study, in a wide range of diameter from 2 to 170 μm was investigated showing that diameter change significantly affected migratory patterns of epithelial cells. Cells behavior on very thick fibers is very similar to observed behavior on 2D scaffolds. Cell morphology was not affected by the incorporation of CNTs (Fig. 4g, 4h, 4i), even when they were in the proximity of formed beads [40].

Since SEM micrographs only reveal information about the cellular cortex, we tracked cellular growth and the health of cellular processes on the nanofibers using light microscope. Keratinocytes that were grown on the control surface showed a cuboidal morphology as expected (Figure 5), similar to previous studies with HaCaT cells [41]. On the other hand, keratinocytes that were grown on nanofibers were more elongated in fiber directions, similar to fibroblastic cells (Figure 5). Cells can sense and adapt to mechanical loads in the form of either acceleration/displacement [42, 43] or substrate stiffness [44]. Our results suggest that HaCaT cells preferred PAN/PPy fibers in early culture compared to coverslip and they continued to proliferate in the vicinity of fibers, while cells seeded on glass surface spread and covered the whole coverslip surface.

PAN/PPy nanofibrous scaffold was found to be a three-dimensional cellular matrix. After 7 days of culture, keratinocytes started to migrate through the fibers and grow under layers of the fibers [45]. It was seen from Fig. 6.c, it caused a significant change in shape of cells. Size of nuclei in fiber-embedded keratinocytes appeared smaller compared to control cells. Their shapes were not circular after 7 days of culture. This indicated that nanofibrous scaffold caused a morphological change.

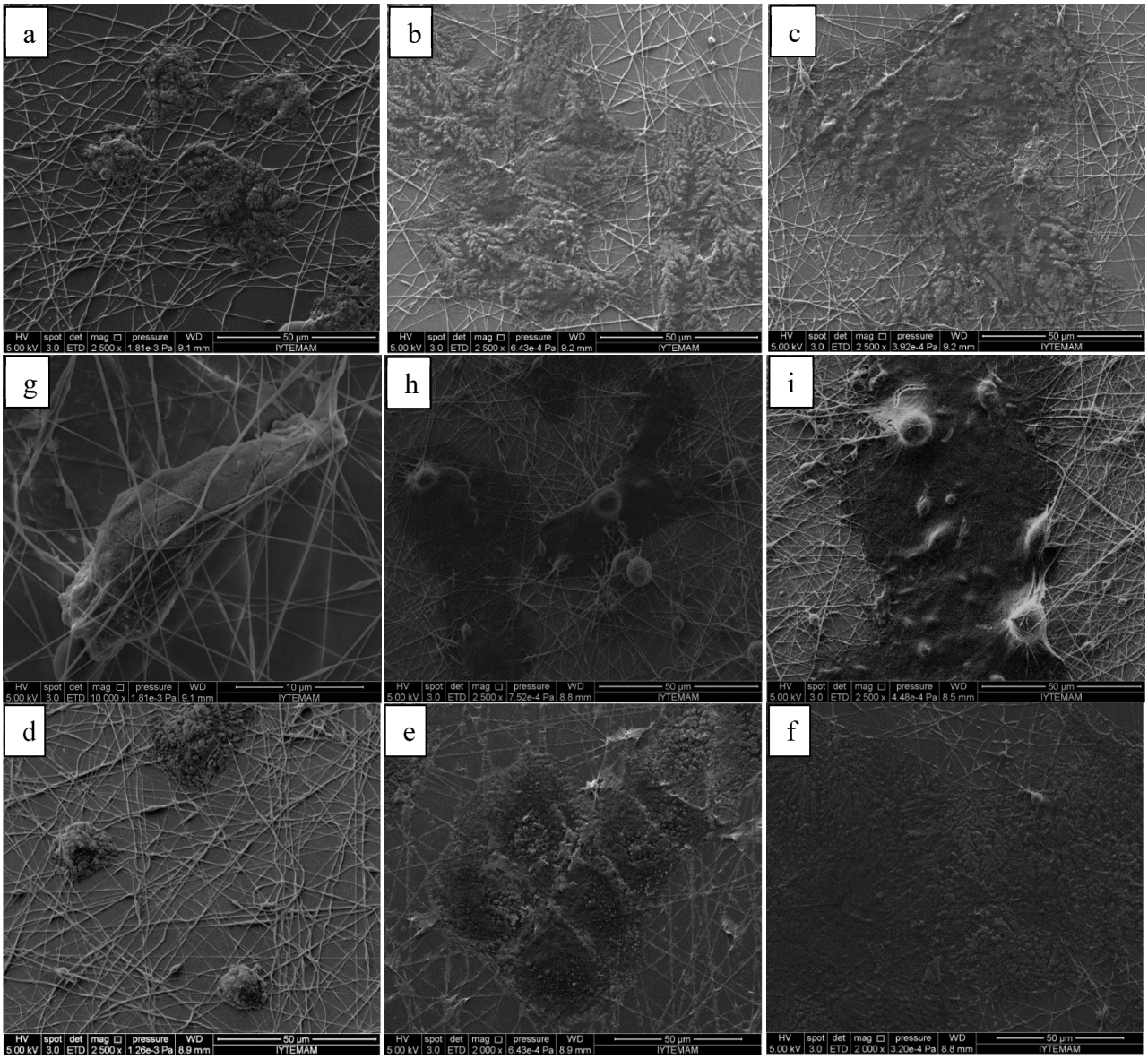

Figure 4 SEM images of skin cells seeded on electrospun PAN/PPy nanofibers containing 10 wt% PPy after a) 1 day, b) 3 days, and c) 7 days of culture, 25 wt% PPy after keeping in cell culture for d) 1 day, e) 3 days, f) 7 days, 10 wt% PPy and 1 wt% CNT after keeping in cell culture for g) 1 day, h) 3 days, i) 7 days. Scale bars 50 μm.

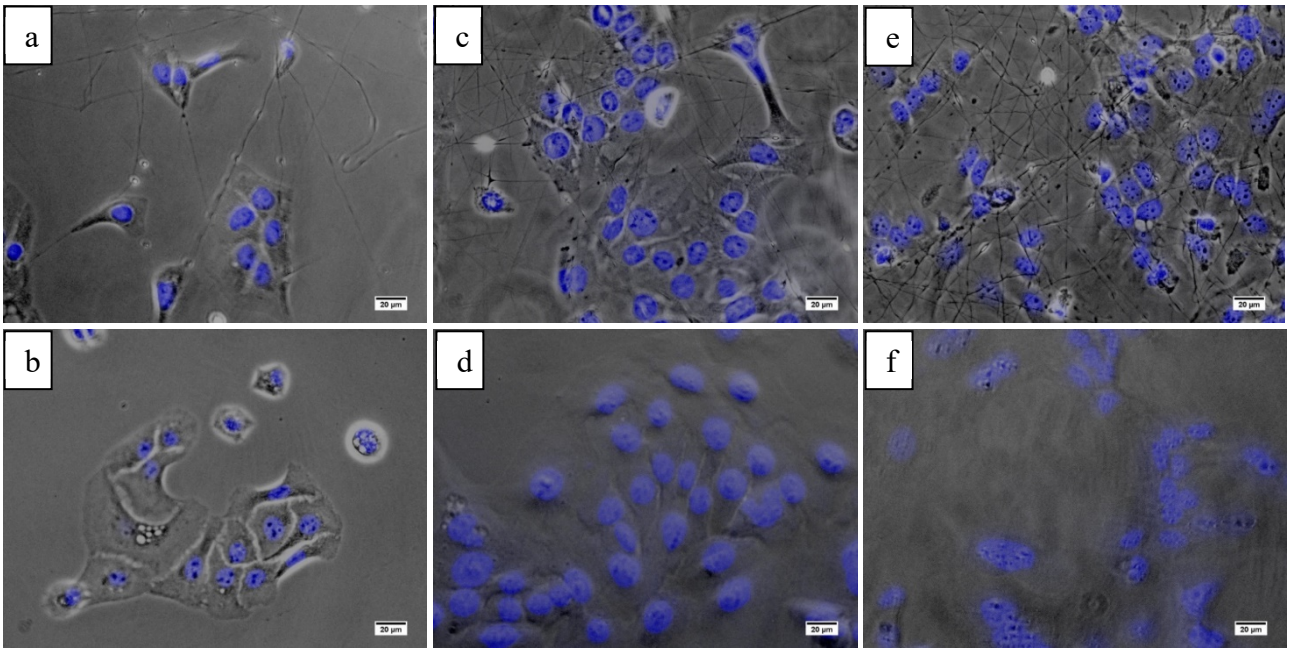

Figure 5 Fluorescence microscopy images of skin cells seeded on electrospun PAN/PPy nanofibers (10 wt% PPy) after a) 1 day, c) 3 days, e) 7 days of culture and their glass control after b) 1 day d) 3 days f) 7 days of culture. Scale bars 20 µm.

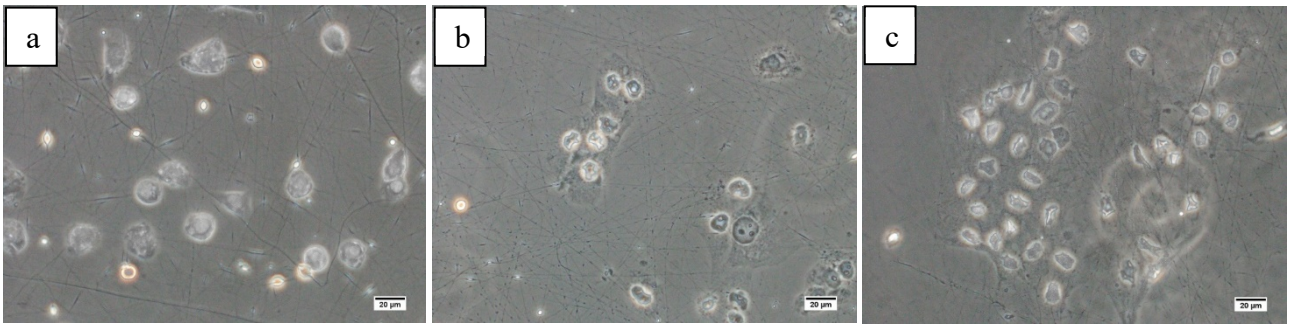

Figure 6 Phase-contrast microscopy images of skin cells seeded on electrospun PAN/PPy nanofibers (25 wt% PPy) after a) 1 day, b) 3 days, c) 7 days of culture. Scale bars 20 µm.

CNT were used to enhance the electrical conductivity and strength of polymeric scaffolds in many studies [46-48] and it is found that they could provide cell attachment and proliferation as tissue engineering scaffolds [48, 49]. Keratinocyte adaptation to CNT incorporated PAN/PPy nanofibers were also tested. We observed that keratinocytes were able to adhere and slide in between the 1 wt% CNT incorporated 10% wt PPy fiber mesh (Fig. 4g, 4h, 4i).

Fluorescent micrographs revealed that in one week of culture keratinocytes reached to confluency on coverslips in a 2D manner, while keratinocytes on CNT incorporated PPy showed a tighter and 3D cellular organization as evidenced by phalloidin staining (Fig. 7). This behavior of keratinocytes on PAN/PPy/CNT nanofibers also differed from their growth on PPy nanofibers without CNT incorporation.

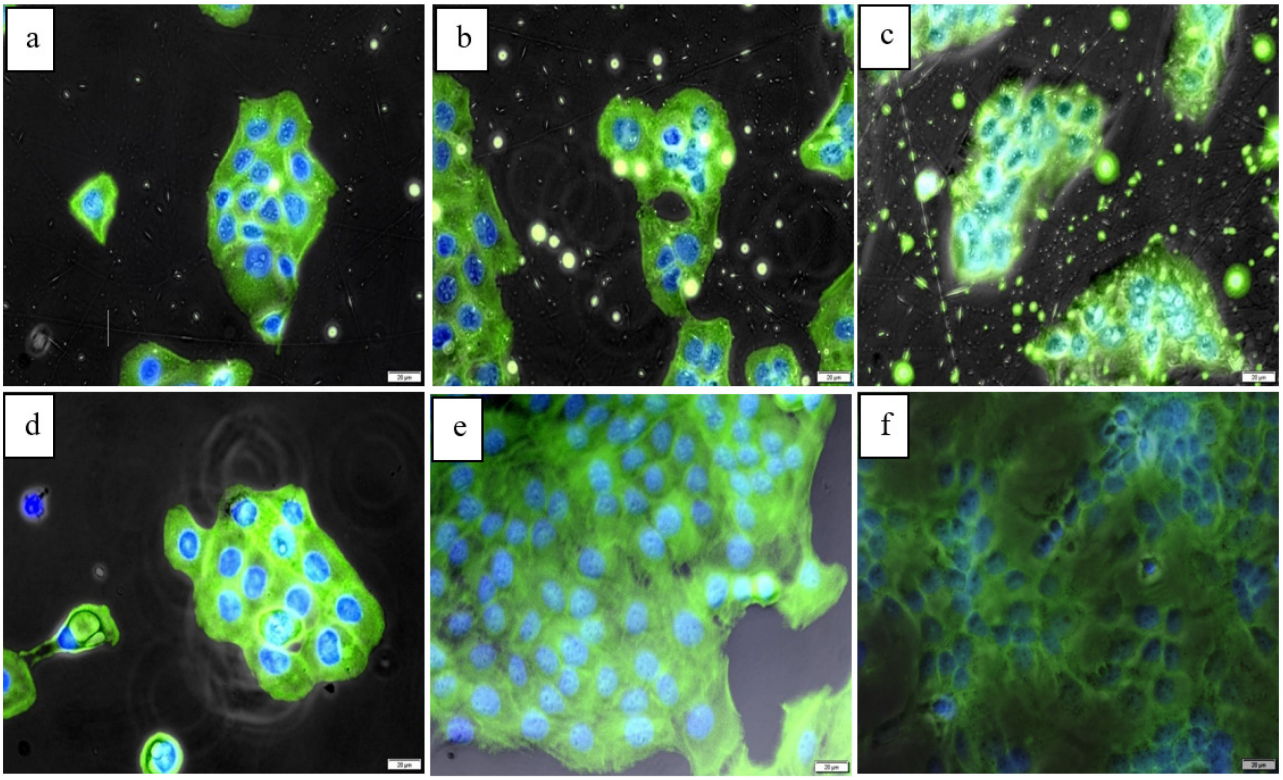

Figure 7 Fluorescence microscopy images of keratinocytes seeded on electrospun PAN/PPy nanofibers (10 wt% PPy) containing 1 wt% CNT after a) 1 day, b) 3 days, c) 7 days of culture and their glass control after d) 1 day, e) 3 days, f) 7 days of culture. Scale bars 20 µm.

The viability of keratinocytes on fabricated nanofibers were examined for one week using MTT assay (Fig. 8). Cells showed a tenfold increase during their 7 days on glass coverslip. A similar increase ($p>0.05$) was observed for keratinocytes that were growing on CNT incorporated PPy, suggesting that fibers even though affecting the morphology, accumulation and the structuring of cells had not interfered with proliferation or showed any cytotoxicity. Our results showed that there is a relationship between the conductivity of nanofibers and viability of keratinocytes. The highest viability was observed for 25 wt% PPy while the lowest value was observed for 10 wt% PPy. These values were inversely proportional with resistance values of nanofibers. It indicated that keratinocytes viability were positively affected by electrical conductivity.

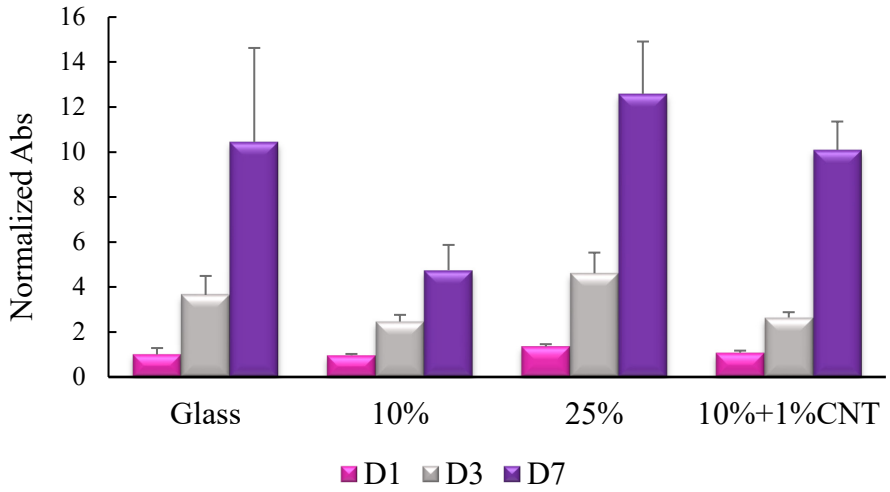

Figure 8 MTT assay of keratinocytes seeded on PAN/PPy nanofibers containing 10 wt% PPy, 25 wt% PPy and 10 wt% PPy and 1 wt% CNT nanofibers after 1,3 and 7 days of culture.

PPy is one of the most extensively investigated polymer for use as tissue engineering scaffolds because of its biocompatibility and high conductivity and it was analyzed for growth of various cell types. It was also examined for human keratinocytes in film form by Davidson et al. and PPy composite films were found attractive candidates for keratinocytes because they were electrically addressable with the potential to both direct and report on cell activity [50]. In this study, we presented that electrospun PAN/PPy nanofibers enabled effective cell adhesion and proliferation for keratinocytes with their 3D structure. PPy concentration altered the diameter of nanofibers where the diameter of nanofibers decreased with increasing PPy content as reported in the literature [6, 51, 52]. Furthermore, the diameter of PAN/PPy nanofibers did not significantly affect the morphology of cells in our study. However, it was reported that thinner electrospun PVA nanofibers led to a more rounded keratinocyte morphology compared to the thicker nanofibers [25].

Our results are consistent with other investigations about electrospun nanofibrous scaffolds; they are appropriate substrates for cell attachment and proliferation. 3D structure of electrospun scaffolds provide larger surface area for cell growth and enhance the cell proliferation [53-55]. However, in literature, it was found that the shape of cells grown on electrospun nanofibrous scaffolds showed some differences from the cell grown on 2D control surfaces [56]. Our results demonstrated that shape of keratinocytes grown on PAN/PPy nanofibers were different from keratinocytes grown on glass control surface. They were stuck among nanofibers with increasing culture time, therefore, they were not circular after 7 days of culture and they were smaller than cells grown on glass.

5. Conclusion

Conductive PAN/PPy nanofibers were synthesized by electrospinning method and their biocompatibility was investigated by utilizing them as keratinocyte scaffold. Two different PPy concentrations were examined and straight and regular nanofibers were obtained. It was observed that with increasing the amount of PPy, diameter of nanofibers reduced. Further, when CNT was incorporated into PAN/PPy solution, beads were observed on the nanofibers and surface morphology became irregular. Cell attachment and proliferation were investigated on these nanofibrous scaffolds. It was found that the diameter of nanofibers did not influence the cellular morphology. However, growing among nanofibers affected the morphology of cells, CNTs reinforced polymeric scaffolds have not been examined yet for keratinocytes in the current literature. In this study, we indicated that CNTs did not affect the biocompatibility of PAN/PPy nanofibers and adhesion and proliferation of keratinocytes occurred on PAN/PPy/CNT scaffold. In the present study, conductive and biocompatible PAN/PPy and PAN/PPy/CNT nanofibrous scaffolds were synthesized for keratinocytes growth and it was found that these synthetic scaffolds could provide an appropriate growth surface for these cells.

References

[1] W.J. Li,C.T. Laurencin,E.J. Caterson,R.S. Tuan,F.K. Ko, Electrospun nanofibrous structure: a novel scaffold for tissue engineering, Journal of Biomedical Materials Research: An Official Journal of The Society for Biomaterials, The Japanese Society for Biomaterials, and The Australian Society for Biomaterials and the Korean Society for Biomaterials, 60 (2002) 613-621.

[2] W.J. Li,C.T. Laurencin,E.J. Caterson,R.S. Tuan,F.K. Ko, Electrospun nanofibrous structure: a novel scaffold for tissue engineering, Journal of biomedical materials research, 60 (2002) 613-621.

[3] N.M. Alves,I. Pashkuleva,R.L. Reis,J.F. Mano, Controlling cell behavior through the design of polymer surfaces, Small, 6 (2010) 2208-2220.

[4] A. Nur-E-Kamal,I. Ahmed,J. Kamal,M. Schindler,S. Meiners, Three dimensional nanofibrillar surfaces induce activation of Rac, Biochemical and biophysical research communications, 331 (2005) 428-434.

[5] H. Yoshimoto,Y. Shin,H. Terai,J. Vacanti, A biodegradable nanofiber scaffold by electrospinning and its potential for bone tissue engineering, Biomaterials, 24 (2003) 2077-2082.

[6] D. Kai,M.P. Prabhakaran,G. Jin,S. Ramakrishna, Polypyrrole-contained electrospun conductive nanofibrous membranes for cardiac tissue engineering, Journal of biomedical materials research Part A, 99 (2011) 376-385.
[7] J.Y. Lee,C.A. Bashur,A.S. Goldstein,C.E. Schmidt, Polypyrrole-coated electrospun PLGA nanofibers for neural tissue applications, Biomaterials, 30 (2009) 4325-4335.
[8] K.J. Gilmore,M. Kita,Y. Han,A. Gelmi,M.J. Higgins,S.E. Moulton,G.M. Clark,R. Kapsa,G.G. Wallace, Skeletal muscle cell proliferation and differentiation on polypyrrole substrates doped with extracellular matrix components, Biomaterials, 30 (2009) 5292-5304.
[9] J.D. Madden,N.A. Vandesteeg,P.A. Anquetil,P.G. Madden,A. Takshi,R.Z. Pytel,S.R. Lafontaine,P.A. Wieringa,I.W. Hunter, Artificial muscle technology: physical principles and naval prospects, IEEE Journal of oceanic engineering, 29 (2004) 706-728.
[10] L. Bay,K. West,P. Sommer-Larsen,S. Skaarup,M. Benslimane, A conducting polymer artificial muscle with 12% linear strain, Advanced Materials, 15 (2003) 310-313.
[11] S. Hara,T. Zama,W. Takashima,K. Kaneto, TFSI-doped polypyrrole actuator with 26% strain, Journal of Materials Chemistry, 14 (2004) 1516-1517.
[12] I.-H. Chen,C.-C. Wang,C.-Y. Chen, Fabrication and structural characterization of polyacrylonitrile and carbon nanofibers containing plasma-modified carbon nanotubes by electrospinning, The Journal of Physical Chemistry C, 114 (2010) 13532-13539.
[13] W. Zheng,J.M. Razal,P.G. Whitten,R. Ovalle-Robles,G.G. Wallace,R.H. Baughman,G.M. Spinks, Artificial muscles based on polypyrrole/carbon nanotube laminates, Advanced materials, 23 (2011) 2966-2970.
[14] J.D. Madden, N.A. Vandesteeg, P.A. Anquetil,P.G. Madden,A. Takshi,R.Z. Pytel,S.R. Lafontaine, P.A. Wieringa,I.W. Hunter, Artificial muscle technology: physical principles and naval prospects, Oceanic Engineering, IEEE Journal of, 29 (2004) 706-728.
[15] M. Sun,S. Zhang,T. Jiang,L. Zhang,J. Yu, Nano-wire networks of sulfur–polypyrrole composite cathode materials for rechargeable lithium batterie,. Electrochemistry Communications, 10 (2008) 1819-1822.
[16] D. Zhang,X. Zhang,Y. Chen,P. Yu,C. Wang,Y. Ma, Enhanced capacitance and rate capability of graphene/polypyrrole composite as electrode material for supercapacitors, Journal of Power Sources, 196 (2011) 5990-5996.
[17] J. Wang,Y. Xu,X. Chen,X. Sun, Capacitance properties of single wall carbon nanotube/polypyrrole composite films, Composites Science and Technology, 67 (2007) 2981-2985.
[18] V.N. Popov, Carbon nanotubes: properties and application, Materials Science and Engineering: R: Reports, 43 (2004) 61-102.
[19] S. Zhang,N. Zhang,C. Huang,K. Ren,Q. Zhang, Microstructure and Electromechanical Properties of Carbon Nanotube/Poly (vinylidene fluoride—trifluoroethylene—chlorofluoroethylene) Composites, Advanced Materials, 17 (2005) 1897-1901.
[20] G.M. Spinks,V. Mottaghitalab,M. Bahrami-Samani,P.G. Whitten,G.G. Wallace, Carbon-Nanotube-Reinforced Polyaniline Fibers for High-Strength Artificial Muscles, Advanced Materials, 18 (2006) 637-640.
[21] M. Tahhan,V.-T. Truong,G.M. Spinks,G.G. Wallace, Carbon nanotube and polyaniline composite actuators*, Smart Materials and Structures, 12(2003) 626.
[22] B.S. Harrison,A. Atala, Carbon nanotube applications for tissue engineering, Biomaterials, 28 (2007) 344-353.
[23] H. Lee,H. Kim,M.S. Cho,J. Choi,Y. Lee, Fabrication of polypyrrole (PPy)/carbon nanotube (CNT) composite electrode on ceramic fabric for supercapacitor applications, Electrochimica Acta, 56 (2011) 7460-7466.
[24] L. Ji,Y. Yao,O. Toprakci,Z. Lin,Y. Liang,Q. Shi,A.J. Medford,C.R. Millns,X. Zhang, Fabrication of carbon nanofiber-driven electrodes from electrospun polyacrylonitrile/polypyrrole bicomponents for high-performance rechargeable lithium-ion batteries, Journal of Power Sources, 195 (2010) 2050-2056.

[25] J. Pelipenko,P. Kocbek,B. Govedarica,R. Rošic,S. Baumgartner,J. Kristl, The topography of electrospun nanofibers and its impact on the growth and mobility of keratinocytes, European Journal of Pharmaceutics and Biopharmaceutics, 84 (2013) 401-411.
[26] H.K. Noh,S.W. Lee,J.-M. Kim,J.-E. Oh,K.-H. Kim,C.-P. Chung,S.-C. Choi,W.H. Park,B.-M. Min, Electrospinning of chitin nanofibers: degradation behavior and cellular response to normal human keratinocytes and fibroblasts, Biomaterials, 27 (2006) 3934-3944.
[27] L. Jeong,I.-S. Yeo,H.N. Kim,Y.I. Yoon,D.H. Jang,S.Y. Jung,B.-M. Min,W.H. Park, Plasma-treated silk fibroin nanofibers for skin regeneration, International Journal of Biological Macromolecules, 44 (2009) 222-228.
[28] B. Dhandayuthapani,U.M. Krishnan,S. Sethuraman, Fabrication and characterization of chitosan-gelatin blend nanofibers for skin tissue engineering, Journal of Biomedical Materials Research Part B: Applied Biomaterials, 94 (2010) 264-272.
[29] S.G. Kumbar,S.P. Nukavarapu,R. James,L.S. Nair,C.T. Laurencin, Electrospun poly (lactic acid-co-glycolic acid) scaffolds for skin tissue engineering, Biomaterials, 29 (2008) 4100-4107.
[30] L. Ji,Z. Lin,A.J. Medford,X. Zhang, Porous carbon nanofibers from electrospun polyacrylonitrile/SiO2 composites as an energy storage material, Carbon, 47 (2009) 3346-3354.
[31] N. Kaur,V. Kumar,S.R. Dhakate, Synthesis and characterization of multiwalled CNT–PAN based composite carbon nanofibers via electrospinning, SpringerPlus, 5 (2016) 483.
[32] C. Luo,J. Wang,P. Jia,Y. Liu,J. An,B. Cao,K. Pan, Hierarchically structured polyacrylonitrile nanofiber mat as highly efficient lead adsorbent for water treatment, Chemical Engineering Journal, 262 (2015) 775-784.
[33] I. Seo,M. Pyo,G. Cho, Micrometer to nanometer patterns of polypyrrole thin films via microphase separation and molecular mask, Langmuir, 18 (2002) 7253-7257.
[34] W. Wang,Y. Zheng,X. Jin,Y. Sun,B. Lu,H. Wang,J. Fang,H. Shao,T. Lin, Unexpectedly high piezoelectricity of electrospun polyacrylonitrile nanofiber membranes, Nano energy, 56 (2019) 588-594.
[35] P. Mavinakuli,S. Wei,Q. Wang,A.B. Karki,S. Dhage,Z. Wang,D.P. Young,Z. Guo, Polypyrrole/silicon carbide nanocomposites with tunable electrical conductivity, The Journal of Physical Chemistry C, 114 (2010): 3874-3882.
[36] J. Hazarika,A. Kumar, Controllable synthesis and characterization of polypyrrole nanoparticles in sodium dodecylsulphate (SDS) micellar solutions, Synthetic Metals, 175 (2013) 155-162.
[37] V. Mottaghitalab,B. Xi,G.M. Spinks,G.G. Wallace, Polyaniline fibres containing single walled carbon nanotubes: Enhanced performance artificial muscles, Synthetic Metals, 156 (2006) 796-803.
[38] S. Canobre,F. Xavier,W. Fagundes,A. de Freitas,F. Amaral, Performance of the chemical and electrochemical composites of PPy/CNT as electrodes in type I supercapacitors, Journal of Nanomaterials, 16 (2015) 160.
[39] C. Guetta-Terrier,P. Monzo,J. Zhu,H. Long,L. Venkatraman,Y. Zhou,P. Wang,S.Y. Chew,A. Mogilner,B. Ladoux, Protrusive waves guide 3D cell migration along nanofibers, J Cell Biol, 211 (2015) 683-701.
[40] R.A. MacDonald,C.M. Voge,M. Kariolis,J.P. Stegemann, Carbon nanotubes increase the electrical conductivity of fibroblast-seeded collagen hydrogels, Acta biomaterialia, 4 (2008) 1583-1592.
[41] A.F. Deyrieux,V.G. Wilson, In vitro culture conditions to study keratinocyte differentiation using the HaCaT cell line, Cytotechnology, 54 (2007) 77-83.
[42] O. Baskan,G. Mese,E. Ozcivici, Low-intensity vibrations normalize adipogenesis-induced morphological and molecular changes of adult mesenchymal stem cells, Proceedings of the Institution of Mechanical Engineers, Part H: Journal of Engineering in Medicine, 231 (2017) 160-168.
[43] L. Demiray,E. ÖZÇİVİCİ, Bone marrow stem cells adapt to low-magnitude vibrations by altering their cytoskeleton during quiescence and osteogenesis, Turkish Journal of Biology, 39 (2015) 88-97.

[44] T. Yeung,P.C. Georges,L.A. Flanagan,B. Marg,M. Ortiz,M. Funaki,N. Zahir,W. Ming,V. Weaver,P.A. Janmey, Effects of substrate stiffness on cell morphology, cytoskeletal structure, and adhesion, Cell motility and the cytoskeleton, 60 (2005) 24-34.
[45] K.S. Rho,L. Jeong,G. Lee,B.-M. Seo,Y.J. Park,S.-D. Hong,S. Roh,J.J. Cho,W.H. Park,B.-M. Min, Electrospinning of collagen nanofibers: effects on the behavior of normal human keratinocytes and early-stage wound healing, Biomaterials, 27 (2006) 1452-1461.
[46] M.C. Serrano,M.C. Gutiérrez,F. del Monte, Role of polymers in the design of 3D carbon nanotube-based scaffolds for biomedical applications, Progress in Polymer Science, 39 (2014) 1448-1471.
[47] P. Gupta,S. Sharan,P. Roy,D. Lahiri, Aligned carbon nanotube reinforced polymeric scaffolds with electrical cues for neural tissue regeneration, Carbon, 95 (2015) 715-724.
[48] M. Kharaziha,S.R. Shin,M. Nikkhah,S.N. Topkaya,N. Masoumi,N. Annabi,M.R. Dokmeci,A. Khademhosseini, Tough and flexible CNT–polymeric hybrid scaffolds for engineering cardiac constructs, Biomaterials, 35 (2014) 7346-7354.
[49] S.-J. Yen,W.-L. Hsu,Y.-C. Chen,H.-C. Su,Y.-C. Chang,H. Chen,S.-R. Yeh,T.-R. Yew, The enhancement of neural growth by amino-functionalization on carbon nanotubes as a neural electrode, Biosensors and Bioelectronics, 26 (2011) 4124-4132.
[50] D.D. Ateh,P. Vadgama,H.A. Navsaria, Culture of human keratinocytes on polypyrrole-based conducting polymers, Tissue engineering, 12 (2006) 645-655.
[51] J. Zheng,A. He,J. Li,J. Xu,C.C. Han, Studies on the controlled morphology and wettability of polystyrene surfaces by electrospinning or electrospraying, Polymer, 47 (2006) 7095-7102.
[52] L. Ji,A.J. Medford,X. Zhang, Electrospun polyacrylonitrile/zinc chloride composite nanofibers and their response to hydrogen sulfide, Polymer,50 (2009) 605-612.
[53] A.S. Goldstein,T.M. Juarez,C.D. Helmke,M.C. Gustin,A.G. Mikos, Effect of convection on osteoblastic cell growth and function in biodegradable polymer foam scaffolds, Biomaterials, 22 (2001) 1279-1288.
[54] W. Mueller-Klieser, Three-dimensional cell cultures: from molecular mechanisms to clinical application,. American Journal of Physiology-Cell Physiology, 273 (1997) C1109-C1123.
[55] H. Hosseinkhani,M. Hosseinkhani,H. Kobayashi, Proliferation and differentiation of mesenchymal stem cells using self-assembled peptide amphiphile nanofibers, Biomedical materials, 1 (2006) 8.
[56] J. Zhong,H. Zhang,J. Yan,X. Gong, Effect of nanofiber orientation of electrospun nanofibrous scaffolds on cell growth and elastin expression of muscle cells, Colloids and Surfaces B: Biointerfaces, 136 (2015) 772-778.